Influence of deposition voltage on tribological properties of W-WS_2 coatings deposited by electrospark deposition

T. X. Liu[a], C. A. Guo[a,*], F. S. Lu[b], X. Y. Zhang[a,c], L. Zhang[b], Z. J. Wang[a], Z. Y. Xu[a], G. L. Zhu[a]
[a]*School of Equipment Engineering, Shenyang Ligong University, Shenyang 110159, China*
[b]*North Huaan Industry Group Co. Ltd, Qiqihaer 161046, China*
[c]*School of Service, Yingkou Modern Service College, Yingkou 115000, China*

Electrospark deposition coatings were prepared with different deposition voltage on CrNi3MoVA steel substrates by using a W-WS_2 sintered electrode and their tribological properties were investigated. The microhardness, roughness and tribological properties of the coatings were tested by using Vickers hardness tester, confocal laser scanning microscope and tribometer, and the morphologies, composition and phase structure were obtained by utilizing scanning electron microscopy (SEM), energy dispersive X-ray spectrum (EDS) and X-ray diffraction(XRD). The results showed that with the increase of deposition voltage, the hardness and roughness of the coatings increase. The coatings remarkably increase the tribological properties of CrNi3MoVA steel, and among the three coatings deposited at 40 V, 60 V and 80 V, the coating deposited at 60 V has the smallest friction coefficient and the best wear resistance.

(Received August 4, 2023; Accepted October 19, 2023)

Keywords: Electrospark deposition, W-WS_2 coating, Tribological properties

1. Introduction

Wear on a sliding or rolling surface can cause premature failure of some key component in an equipment, and then improper working for the equipment. On the basis of some estimates, losses resulting from wear can reach approximate 4% of its gross national product (GNP) in the United States [1]. Therefore, the significance of friction reduction and wear resistance increase can never be underestimated for economic development and long-time equipment operation reliability. The effective application of tribological knowledge can save about 1% of GNP in an industrialized country, and the savings are expected to attain an order of 50 times the research expenditure.

As wear always takes place on a part surface, the coatings with transition metal dichalcogenides are generally deposited on the part surface to improve its tribological properties [2-3]. However, the friction coefficient and wear rate of transition metal dichalcogenides will increase sharply in humid air for the dangling or unsaturated bonds on the edge of basal planes react with moisture and oxygen in ambient environment, which will lead to the coating degradation. To address this issue, there have been many investigations in regard to doping metal or oxide in transition metal dichalcogenides to improve their tribological properties in air. The dopants, such as Cu [4-5], Ni [2, 6], Al [7], etc., can remarkably increase coating mechanical properties and oxidation resistance.

Electrochemical depostion [8], electrodeposition [9], thermal spraying [10], laser cladding [11] and electrospark deposition (ESD) [2, 6, 12] have been utilized to prepare coatings with transition metal dichalcogenides. Compared with the other four techniques, the coatings prepared by ESD possess much stronger metallurgical bonding with the substrate, and moreover the substrate has no distortion or metallurgical change due to low heat effect during ESD process. Moreover, ESD coatings always consist of nanoscaled structure due to the rapid cooling speed that can attain on the order of 10^5-10^6 K/s, which can make the coatings have improved properties [2, 6,

* Corresponding author: bigocean1979@aliyun.com
https://doi.org/10.15251/CL.2023.2010.741

13]. In addition, ESD is also a simple, cost-effective, and environment-friendly technique applied in the field of aerospace, chemistry, machinery, military, etc. [14-15] Recently C. Guo, et al. [2] investigated the performance of friction and wear of the Ni-MoS_2 coatings prepared by ESD, showing that the Ni-MoS_2 coating possesses excellent tribological properties due to the synergistic effect of MoS_2 and MoO_2 in the coating. Wang S, et al. [6] used a Ni-WS_2 sintered electrode to prepare a coating on a CrNi3MoVA steel substrate by employing ESD technique, showing that the Ni-WS_2 coating also exhibits outstanding tribological properties due to its friction coefficient and wear rate reduction about 79% and 96% in contrast to the CrNi3MoVA steel, respectively. Both research results suggest that ESD technique has a promising prospect for preparing coatings with transition metal dichalcogenides.

Compared with Ni, Tungsten (W) has higher ultimate tensile strength, hardness and fracture toughness, thus it is usually used as military swaging rod for armor piercing in military. To the best knowledge of the authors, there is still no relevant research report about a W-WS_2 coating prepared by ESD technique. Moreover, deposition parameters have substantial influence on the ESD coating performance [16-17]. Hence, in this work, the influence of deposition voltage on the tribological properties of W-WS_2 coating prepared by ESD will be investigated.

2. Materials and methods

The substrate material used in this experiment is CrNi3MoVA steel, and its chemical composition is shown in Table 1. The CrNi3MoVA steel bar was cut into rectangular samples in a size of 20 mm×10 mm×4 mm by wire cutting. The cut samples were polished with SiC sandpaper to 2000 # and then polished with 2.5 μm diamond paste. The polished samples were ultrasonically cleaned in anhydrous ethanol for 10 min and then blown dry. The electrode material is made of W and WS_2 powder with a purity of more than 99%, and the average particle size of the powder is approximately 2 μm. In this experiment, the W-WS_2 composite material was prepared by spark plasma sintering (SPS) technique through mixing W and WS_2 powders in predetermined proportion (15% WS_2 powder, 85% W powder). The composite W-WS_2 material is cut to form a cylindrical electrode with a size of Φ 5 mm×50 mm, and polished to 800# by using SiC sandpaper to remove the oxide layer from the surface, and then also cleaned in anhydrous ethanol for 10 min, and blown dry. A DJ-2000 adjustable power metal surface repair machine was used as ESD equipment, and the electrode material was clamped by the fixture in the deposition gun and extended a length of 20 mm, and the W-WS_2 coating was prepared on the substrate surface under argon protection. Three deposition voltages were used to deposit the coatings in order to investigate the influence of deposition voltage on the tribological properties of the coatings, and the specific process parameters are shown in Table 2.

Table 1. Chemical composition of CrNi3MoVA steel (Wt %).

C	Mn	Si	Cr	Ni	Mo	V	S	P
0.41	0.41	0.25	1.28	3.14	0.37	0.20	0.001	0.012

Table 2. Process parameters of W-WS_2 coatings.

Voltage/V	Power/W	Electrode rotation speed/r·min^{-1}	Argon flow rate/L·min^{-1}	Unit area deposition time/min·cm^{-2}
40	800	2500	15	1
60	1200	2500	15	1
80	1600	2500	15	1

The surface morphologies as well as the elemental composition of the W-WS_2 coatings were characterized by scanning electron microscope (SEM, TESCAN VEGA3, Czech Republic) equipped with energy dispersive spectrometer (EDS, X-MAX, UK). The phase structure of the coating was characterized by X-ray diffraction (XRD,X 'Pert PRO, Hollad). The three-dimensional morphologies and surface roughness of the coatings were measured by confocal laser scanning microscope (CLSM, LS4000, Japan). The hardness change of the coating cross-section in the depth direction was measured by Vickers hardness tester (FM810, Japan), and the friction and wear tests of W-WS_2 coatings with different deposition voltage were carried out at room temperature by using HSR-2M reciprocating friction and wear tester. The friction pair was a 304 stainless steel ball with a diameter of 6 mm, and the parameters of the friction and wear test are shown in Table 3. At the end of the test, the sample was ultrasonically cleaned with anhydrous ethanol for 10 min, and it was weighed before and after friction and wear test by using a high-precision electronic balance to measure weight loss.

Table 3. Friction and wear test parameters.

Reciprocation distance/mm	Loading power/N	Running time/min	Reciprocation times/t·min^{-1}
5	3	10	500

3. Results and discussion

3.1. Microstructure and phase structure of W-WS_2 coatings

Fig. 1 shows the surface morphologies of W-WS_2 coatings deposited at 40 V (a), 60 V (b) and 80 V (c). As shown in Fig. 1, there are many globes with a size of micron order on the surface of W-WS_2 coatings, which is different from the splashing and overlapping feature of the surface morphology of ESD Ni-WS_2 coating [6].

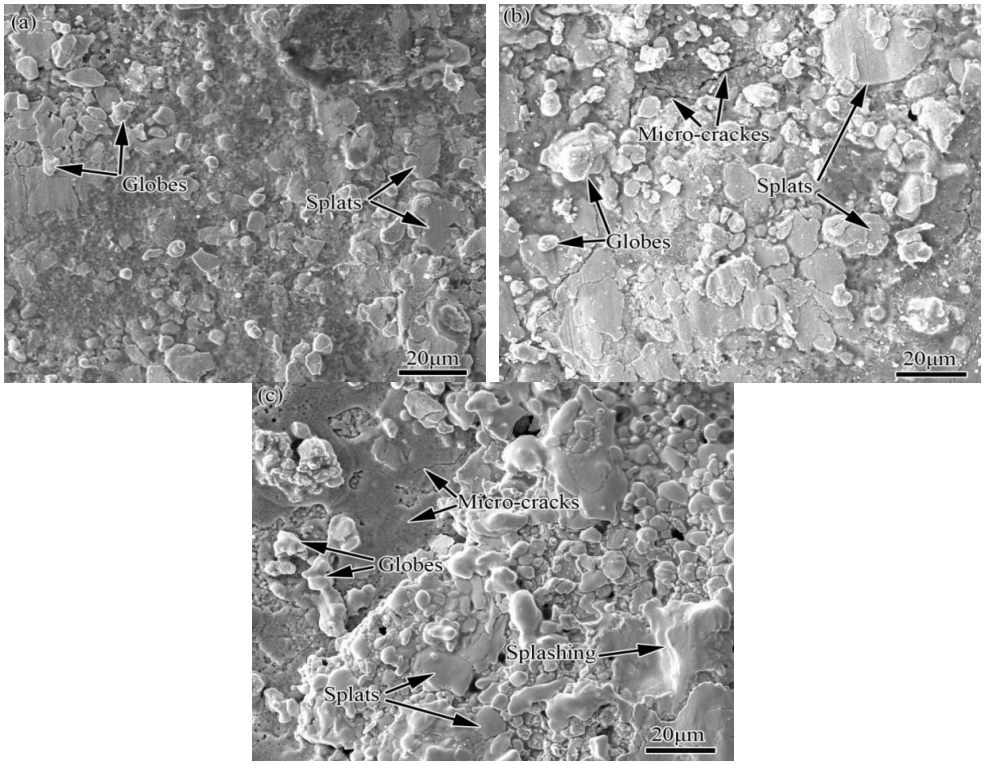

Fig. 1. Surface morphologies of W-WS_2 coatings deposited at 40V (a), 60V (b) and 80V (c).

The reason could be related with the melting points for W (3410 ℃) has a much higher melting point than Ni (1453 ℃), and it have less time to splash before solidifying. Moreover, with the increase of deposition voltage, the size of the splats on the coating surface becomes bigger, and when the deposition voltage is 80 V, the splashing feature appears on the coating surface. In addition, there are few cracks on the coating surface deposited at 40 V while several micro-cracks due to thermal stress during rapid heating and cooling in the ESD process can be observed on the coating surface deposited at 60 V and 80 V. Table 4 shows the EDS quantitative results covering the whole surface (Fig. 1) at different deposition voltage. As shown in Table 4, with the increase of deposition voltage, the content of W obviously increases while that of Fe correspondingly decreases, and it's worth noting that the content of S firstly mildly increases and then remarkably decreases.

Table 4. EDS quantitative results covering the whole surface (Fig. 1) at different deposition voltage (At %).

Voltage/V	Elements				
	W	S	Fe	Ni	Cr
40	60.40	11.20	28.18	0	0.23
60	69.59	12.87	17.03	0	0.52
80	79.63	5.46	14.49	0	0.43

Fig. 2 shows the XRD patterns of the W-WS_2 coatings at different deposition voltage. As shown in Fig. 2, the W-WS_2 coatings mainly consist of α-W and WS_2, which agrees with the EDS results of the coatings. As the ESD process was carried out under argon protection, the coating did not undergo significant oxidation, which was also verified by the absence of oxide phases in the XRD patterns.

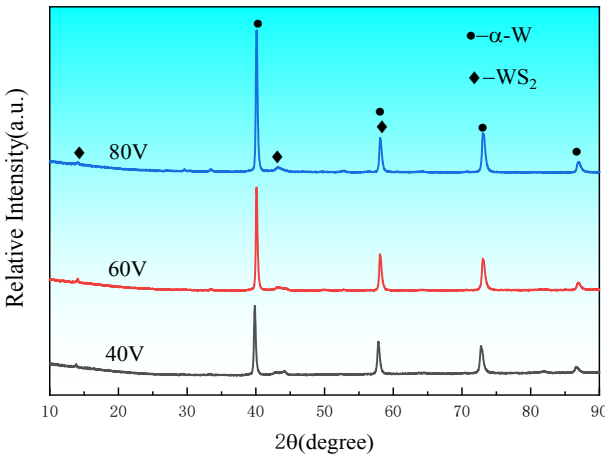

Fig. 2. XRD patterns of W-WS_2 coatings at different deposition voltage.

3.2. Surface roughness of W-WS_2 coatings

Fig. 3 shows the three-dimensional morphologies of the W-WS_2 coatings under different deposition voltage, and Fig. 4 shows the results of surface roughness measurement. As shown in Fig. 3 and Fig. 4, with the increase of deposition voltage, the roughness correspondingly linearly increase. The roughness results indicated that the splashing feature deposited at 80 V have no influence on the surface roughness.

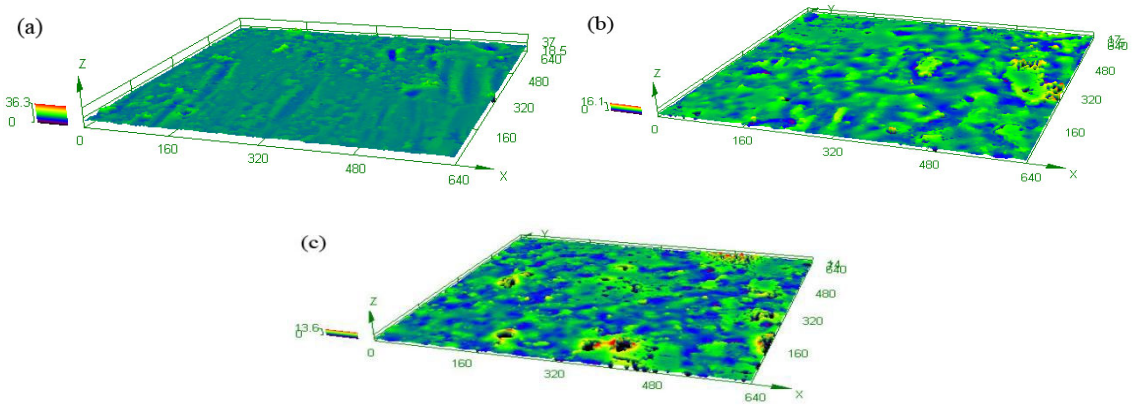

Fig. 3. Three-dimensional surface morphologies: (a) 40V, (b) 60V, (c) 80V.

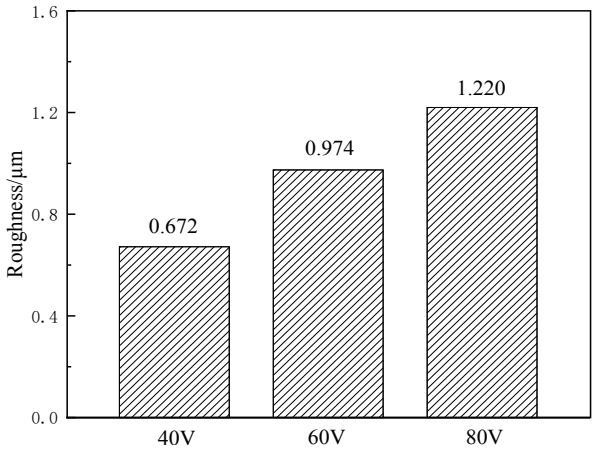

Fig. 4. Results of roughness measurement on W-WS_2 coating surface with different deposition voltage.

3.3. Microhardness of W-WS_2 coatings

Fig. 5 shows the microhardness distribution along the depth direction in the cross-section of W-WS_2 coatings at different deposition voltage. As shown in Fig. 5, with the increase of deposition voltage, the hardness of the coating increases. Among the three coatings deposited at different voltage, the highest hardness of the coating deposited at 80 V is 658.7 HV. Furthermore, the hardness of the three coatings reduces from the top of the coating to the substrate along the depth direction in the cross-section of W-WS_2 coatings due to the gradient coating generally formed by ESD technology [2, 6]. At the top of the coating in the cross-section, the content of W is much more and that of Fe is much less according to the EDS results (Table 4), so the top of the coating has the highest hardness along the depth direction. For the same reason, with the increase of deposition voltage, the content of W increase on the surface of the coating, thus the coating deposited at 80 V has the highest hardness. It is also can be observed from Fig. 5 that the thickness of the coating deposited at 40 V is the thinnest among the three coatings for its hardness approximates to the hardness of CrNi3MoVA steel at the last two test points.

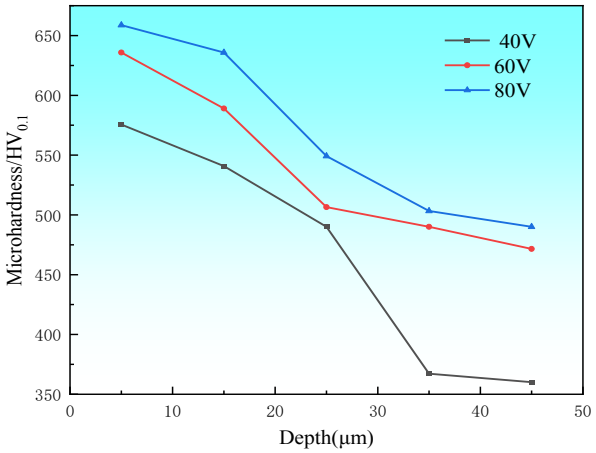

Fig. 5. Microhardness distribution along the depth direction in the cross-section of W-WS_2 coatings at different deposition voltage.

3.4. Friction and wear behavior

Fig. 6 shows the worn morphologies of CrNi3MoVA steel and W-WS_2 coatings with different deposition voltage. As shown in Fig. 6(a), there are furrows on the worn surface of CrNi3MoVA steel, and beside the furrows severe plastic deformation of material takes place. Moreover, shear fracture can also be observed at the edge of the deformed material. Therefore the wear mechanism of CrNi3MoVA steel can be characterized as severe adhesive wear. In contrast to the CrNi3MoVA steel, the worn morphologies of W-WS_2 coatings display a different feature (Fig. 6(a)-(c)). Comparing with the splats distributed on the surface of the as-deposited W-WS_2 coatings, the worn surface of the three coatings becomes more smooth except for several light scratches. Thus the mechanism of W-WS_2 coatings all belongs to abrasive wear.

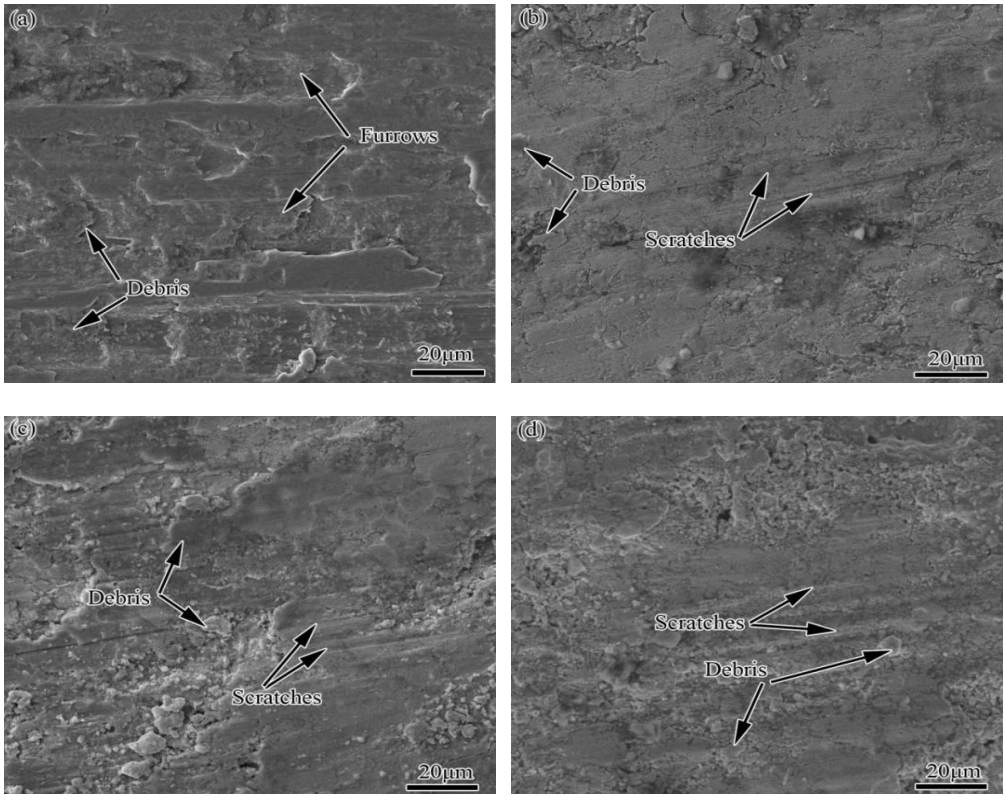

Fig. 6. Worn morphologies of CrNi3MoVA steel (a) and W-WS_2 coatings deposited at 40V (b), 60V (c) and 80V (d).

Fig. 7 shows the friction coefficients of CrNi3MoVA steel and W-WS_2 coatings under different pulse energy. As shown in Fig. 7, the CrNi3MoVA steel has the biggest friction coefficient, floating in the interval of 1.04 to 1.34; the friction coefficient of W-WS_2 coating deposited at 60V is the smallest, and its fluctuation is also the smallest, stabilizing at about 0.5; the friction coefficient of W-WS_2 coating deposited at 80V is between 0.6 and 0.75; it can be found that the friction coefficient of W-WS_2 coating deposited at 40V is very low (about 0.24) at the initial stage, and then it grows and finally stabilizes between 0.8 and 1.0 after 1min.

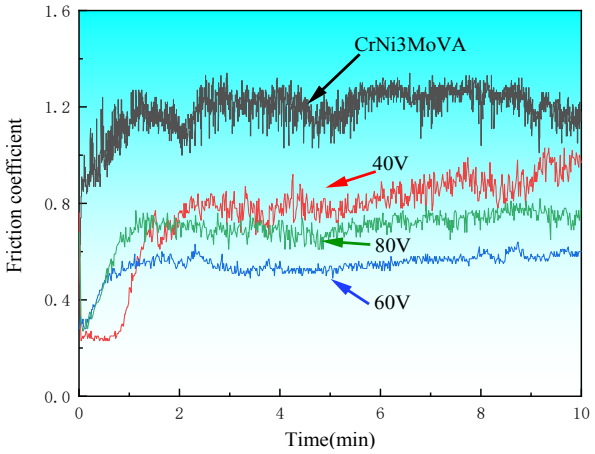

Fig. 7. Friction coefficients of CrNi3MoVA steel and W-WS_2 coatings under different deposition voltage.

Fig. 8 shows the weight loss of CrNi3MoVA steel and W-WS_2 coatings deposited at different deposition voltage. As shown in Fig. 8, in contrast to the weight loss of CrNi3MoVA steel, the W-WS_2 coatings all increase the wear resistance of the CrNi3MoVA steel. Among the three coatings, the W-WS_2 coating deposited at 60 V has the best wear resistance, and its weight loss is only one third of the coating deposited at 80 V and one fifth of the coating deposited at 40 V, respectively, and reduced 95% than the CrNi3MoVA steel.

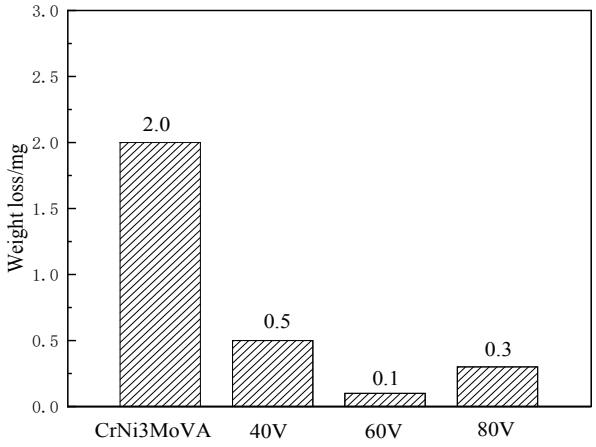

Fig. 8. Weight loss of CrNi3MoVA steel and W-WS_2 coatings deposited at different deposition voltage.

The pulse energy is controlled by the deposition voltage and discharge capacitance together, and it can be calculated by Equation [18].

$$E=1/2CV^2 \quad (1)$$

where E is pulse energy, C is discharge capacitance, and V is deposition voltage. In this experiment, the value of C is a constant, so E is determined only by V. Moreover, V is a quadratic component, thus the change of V will have a significant influence on E. With the increase of deposition voltage, the transfer mass from the electrode will augment at one pulse time, and the more the transfer mass, the more time the melting pool solidify, so the splashing feature appears when the deposition voltage was 80 V. In addition, with the increase of transfer mass, the coating surface roughness becomes bigger and the content of W on the surface of the coating also increases. However, as WS_2 has a low decomposition temperature (783 K), it has more time to decompose when the deposition voltage is 80 V, so the content of S is much less than the coating deposited at 40 V and 60 V, which indicated that the WS_2 phase in the coating will decrease. These results are well agreement with the friction coefficient results for the friction coefficient of the coating deposited at 60 V is smaller than that of the coating deposited at 80 V. It is worth noting that the friction coefficient of the coating deposited at 40 V is bigger than that of the coating deposited at 80 V mainly because the coating deposited at 40 V is the thinnest and has the lowest hardness.

According to Archard equation [19]

$$V=\mu LN/H \tag{2}$$

where V is worn volume, μ is friction coefficient, L is sliding distance, N is applied load, and H is hardness. In Equation (2) L and N are the fixed value, and V is determined by both μ and H. Among the three coatings deposited at different voltage, the coating deposited at 60 V has the smallest friction coefficient and higher hardness, and thus processes the best wear resistance. The coating deposited at 80 V has a smaller friction coefficient and a higher hardness than the coating deposited at 40 V, so it has a better wear resistance.

4. Conclusions

The ESD W-WS_2 coatings mainly consist of α-W and WS_2. With the increase of deposition voltage, the size of the splats on the coating surface becomes bigger, and the splashing feature appears when the deposition voltage at 80 V.

The roughness and hardness of the coating increase with the increase of the deposition voltage, and the hardness in the cross-section is of gradient change from the top of the coating to the substrate along the depth direction. The coating remarkably increases the tribological properties of the CrNi3MoVA steel, and its wear mechanism is abrasive wear whilst that of the CrNi3MoVA steel belongs to adhesive wear. Among the three coatings deposited at 40 V, 60 V and 80 V, the coating deposited at 60 V has the smallest friction coefficient and the best wear resistance.

Acknowledgments

The authors are grateful for the financial support of the National Science Foundation of Liaoning Province of China (No.2019-ZD-0264), and the Research Project of application foundation of Liaoning Province of China (No.2022JH2/101300006), and the Supporting Project of Middle-young Aged Innovative Talents of Science and Technology of Shenyang City, and the Research Innovation Team Building Program of Shenyang Ligong University, and the Light-Selection Team Plan of Shenyang Ligong University.

References

[1] T. W. Scharf, P. G. Kotula, S. V. Prasad, Acta Materialia **58**, 4100 (2010); https://doi.org/10.1016/j.actamat.2010.03.040
[2] C. Guo, F. Kong, S. Zhao, X. Yan, J. Yang, J. Zhang, Chalcogenide Letters **16**(7), 309 (2019).

[3] Y. He, S. C. Wang, F. C. Walsh, Y. L. Chiu, P. A. S. Reed, Surface & Coatings Technology **307**, 926 (2016); https://doi.org/10.1016/j.surfcoat.2016.09.078
[4] Y. Sun , Y. Q. Fang, F. Q. Shang, J. Zhang, W. Liu, H. Y. Shen, B. Guo, Powder Technology **422**, 118453 (2023); https://doi.org/10.1016/j.powtec.2023.118453
[5] J. H. Yan, Y. Wang, Y. J. Guo, Journal of Materials Science & Technology **24**, 5420 (2023); https://doi.org/10.1016/j.jmrt.2023.04.114
[6] M. Yue, W. Zhao, S. Wang, J. Li, C. Zhu , H. Jin, C. Guo, Chalcogenide Letters **18**(10), 557 (2021).
[7] P. F. Li, F. Xu, S. Robertson, Z. X. Zhou, X. H. Hou, A. T. Clare, N. T. Aboulkhair, Materials & Design **216**, 110543 (2022); https://doi.org/10.1016/j.matdes.2022.110543
[8] Y. H. Yao, Y. C. Wu, Z. Y. Zhang, H Zhu, M. N. Hu, K. Xu, Y. Liu, Applied Surface Science **605**, 154635 (2022); https://doi.org/10.1016/j.apsusc.2022.154635
[9] Z. X. Chen, J. Wagner, V. Turq, J. Hillairet, P. L. Taberna, R. Laloo, S. Duluard, J. M. Bernard, Y. T. Song, Q. X. Yang, K. Lu, Y. Cheng, Journal of Alloys and Compounds **829**(15), 154585 (2020); https://doi.org/10.1016/j.jallcom.2020.154585
[10] Q. Liu, Y. Wang, Y. Bai, Z. D. Li, M. Y. Bao, H. Zhan, N. Liu, Z. D. Chang, Y. S. Ma, Surface & Coatings Technology **421**, 127383 (2021); https://doi.org/10.1016/j.surfcoat.2021.127383
[11] H. Torres, T. Vuchkovb, S. Slawikc, C. Gachotd, B. Prakashb, M. R. Ripoll, Wear **408**, 22 (2018); https://doi.org/10.1016/j.wear.2018.05.001
[12] T. K. Cao, S. T. Lei, M. Zhang, Surface & Coatings Technology **270**, 24 (2015); https://doi.org/10.1016/j.surfcoat.2015.03.023
[13] H. L. Yang, X. M. Chen, L. Chen, Z. J. Wang, G. C. Hou, C. A. Guo, J. Zhang, Digest Journal of Nanomaterials and Biostructures **18**(1), 145 (2023); https://doi.org/10.15251/DJNB.2023.181.145
[14] C. X. Geng, H. X. Zhang, X. J. Li, H. B. Geng, Materials Science & Engineering A **868**, 144746 (2023); https://doi.org/10.1016/j.msea.2023.144746
[15] K. A. Kuptsov, M. N. Antonyuk, A. N. Sheveyko, A. V. Bondarev, S. G. Ignatov, P. V. Slukin, P. Dwivedi, A. Fraile, T. Polcar, D. V. Shtansky, Surface & Coatings Technology **453**, 129136 (2023); https://doi.org/10.1016/j.surfcoat.2022.129136
[16] M. Salmaliyan, F. M. Ghaeni, M. Ebrahimnia, Surface and Coatings Technology **321**, 81 (2017); https://doi.org/10.1016/j.surfcoat.2017.04.040
[17] H. Shafyei, M. Salehi, A. Bahrami, Ceramics International **46**, 15276 (2020); https://doi.org/10.1016/j.ceramint.2020.03.068
[18] J. Milligan, D. W. Heard, M. Brochu, Applied Surface Science **256**, 4009 (2010); https://doi.org/10.1016/j.apsusc.2010.01.068
[19] J. F. Archard, Journal of Applied Physics **24**(4), 981(1953); https://doi: org/10.1063/1.1721448